

Wave Propagation in Piezoelectric Rods with Rectangular Cross Sections

Xiaoming Zhang¹, Xingxin Xu^{1,2} and Yuqing Wang¹

Abstract: Orthogonal polynomial approach has been used to deal with the wave propagation in structures that have finite dimension in only one direction, such as horizontally infinite flat plates, axially infinite hollow cylinders. In order to solve wave propagation in two-dimensional piezoelectric rod with rectangular cross section, i.e. the piezoelectric plate with finite dimensions in two directions, an extended orthogonal polynomial approach is proposed in this paper. For validation and illustration purposes, the proposed approach is applied to solving the wave propagation in a square steel rod. The results obtained are in good agreement with the results from the semi-analytical finite element method. The dispersion curves and displacement and electric potential distributions of various rectangular piezoelectric rods are calculated, and the effects of the different width to height ratio, material parameters and different polarizing directions on the dispersion curves and displacement and electric potential distributions are discussed.

Keywords: rectangular rod, piezoelectric materials, orthogonal polynomial, wave propagation, dispersion curves, displacement profiles.

1 Introduction

Piezoelectric materials possess the important property of linear coupling between mechanical and electrical fields, which renders them useful in many areas of modern technology. In recent years, piezoelectric materials have been integrated with the structural systems to form a class of smart structures and embedded as layers or fibers into multifunctional composites. Advanced structures with intelligent self-monitoring and self-control capabilities are increasing due to rapid development for smart space systems and micro-electromechanical structures. Piezoelectric materials having electromechanical coupling effects, have found extensive applications

¹ School of Mechanical and Power Engineering, Henan Polytechnic University, Jiaozuo 454003, P.R. China.

² Corresponding Author.

in such smart devices. The behavior of the wave mode selected directly affects the performance of the device. Thus, it is significant to study the wave characteristics in piezoelectric materials.

Theoretical studies on wave propagation in piezoelectric materials have attracted considerable attention. Some are listed here. Paul [Paul et al. (1987)] obtained the frequency equation for a piezoelectric solid cylinder of arbitrary cross section using the Fourier expansion collocation method. Liu [Liu et al. (2003)] analyzed the dispersion of waves and characteristic wave surfaces in plates of functionally graded piezoelectric material with an inhomogeneous layer element method. Ebenezer [Ebenezer et al. (2003)] investigated axially polarized piezoelectric cylinders with arbitrary boundary conditions on the flat surfaces by applying the Bessel series. Chakraborty [Chakraborty (2009)] investigated the propagating nature of the elastic and electric wave in bone and porous piezoelectric media, and solved the governing partial differential equations in the frequency domain by transforming equations into a polynomial eigenvalue structure. Han [Han et al. (2005)] analyzed the dispersion and characteristic surface of waves in a hybrid multilayered piezoelectric plate with an analytical-numerical method. Many researches have studied wave propagation behavior in layered piezoelectric structures with different methods, such as the extended Durbin method [Ing et al. (2013)], the layer element method [Xi et al. (2002); Han et al. (2004)], the reverberation-ray matrix method [Guo et al. (2009)], the transfer matrix method [Cai et al. (2001)], the orthogonal polynomial series method [Yu et al. (2012)] and so on.

To analyze free guided waves in piezoelectric structures, some investigations made a theory using an orthonormal basis set for the expansion of field quantities. It was first applied to line acoustic waves guided in homogeneous semi-infinite wedges and ridges [Maradudin et al. (1972); Sharon et al. (1974)], to surface acoustic waves in layered [Datta et al. (1978); Kim et al. (1990)] and inhomogeneous [Gubernatis et al. (1987)] semi-infinite structures. Later on, by applying Legendre polynomial expansions, the method has been extended to obtain, for finite-thickness structures, the mode spectrum such as Lamb-like waves in multilayered structures [Lefebvre et al. (1999); Yu et al. (2013)] and functionally graded material structures [Lefebvre et al. (2001)]. The polynomial approach has also been applied to piezoelectric-piezomagnetic composites to study the magneto-electric coupling effect in cylinders [Yu et al. (2008)] and plates [Wu et al. (2009)] and spherical curved plates [Yu et al. (2010)].

Although the polynomial approach is versatile in solving wave problem, so far, it can only deal with the wave propagation in one dimension structure, i.e. these structures have finite dimension only in one direction, such as horizontally infinite flat plates, axially infinite hollow cylinders. But in practical applications, many

piezoelectric elements have limited dimensions in two directions. In this paper, an extension of the orthogonal polynomial approach is proposed to solve wave propagation in 2D piezoelectric structures, i.e. piezoelectric rods with rectangular cross sections. Through numerical comparisons with the available result, the validation of the extended polynomial approach is illustrated. Dispersion curves and displacement profiles of various rectangular rods are shown. The effects of the different width to height ratio, material parameters and different polarizing directions on the dispersion curves and displacement and electric potential distributions are also discussed. In this paper, traction free and open circuit boundary conditions are assumed.

2 Mathematics and formulation of the problem

Let us consider an orthotropic rectangular piezoelectric rod of width d and height h . It is infinite in wave propagating direction (x -axis), as shown in Figure 1. Assume that the origin of the Cartesian coordinate system is located at a corner of the rectangular section and the rod lies in the positive $y-z$ region, where the medium occupies the region $0 \leq z \leq h$ and $0 \leq y \leq d$. The body forces and electric charge are assumed to be zero in this paper.

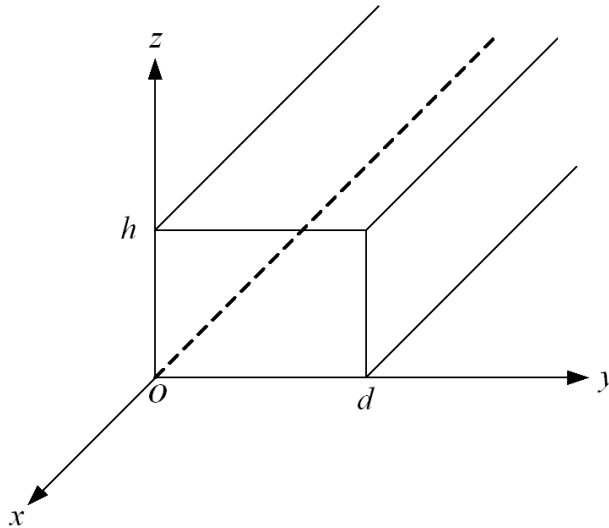


Figure 1: Schematic diagram of a piezoelectric rod with rectangular cross section.

The dynamic equation for the rectangular piezoelectric rod is governed by

$$\begin{aligned}
 \frac{\partial T_{xx}}{\partial x} + \frac{\partial T_{xy}}{\partial y} + \frac{\partial T_{xz}}{\partial z} &= \rho \frac{\partial^2 u_x}{\partial t^2} \\
 \frac{\partial T_{xy}}{\partial x} + \frac{\partial T_{yy}}{\partial y} + \frac{\partial T_{yz}}{\partial z} &= \rho \frac{\partial^2 u_y}{\partial t^2} \\
 \frac{\partial T_{xz}}{\partial x} + \frac{\partial T_{yz}}{\partial y} + \frac{\partial T_{zz}}{\partial z} &= \rho \frac{\partial^2 u_z}{\partial t^2} \\
 \frac{\partial D_x}{\partial x} + \frac{\partial D_y}{\partial y} + \frac{\partial D_z}{\partial z} &= 0
 \end{aligned} \tag{1}$$

where T_{ij} , u_i and D_i are the stress, elastic displacement and electric displacement, respectively; ρ is the density of the material.

The relationship between the general strain and general displacement can be expressed as

$$\begin{aligned}
 \varepsilon_{xx} &= \frac{\partial u_x}{\partial x}, \quad \varepsilon_{yy} = \frac{\partial u_y}{\partial y}, \quad \varepsilon_{zz} = \frac{\partial u_z}{\partial z}, \quad \varepsilon_{yz} = \frac{1}{2} \left(\frac{\partial u_y}{\partial z} + \frac{\partial u_z}{\partial y} \right), \\
 \varepsilon_{xz} &= \frac{1}{2} \left(\frac{\partial u_x}{\partial z} + \frac{\partial u_z}{\partial x} \right), \quad \varepsilon_{xy} = \frac{1}{2} \left(\frac{\partial u_x}{\partial y} + \frac{\partial u_y}{\partial x} \right), \quad E_x = -\frac{\partial \phi}{\partial x}, \\
 E_y &= -\frac{\partial \phi}{\partial y}, \quad E_z = -\frac{\partial \phi}{\partial z},
 \end{aligned} \tag{2}$$

where ε_{ij} , E_i and ϕ are the strain, electric field and electric potential, respectively.

By introducing the function $I(y, z)$, defined as follows,

$$I(y, z) = \begin{cases} 1, & 0 \leq y \leq d \quad \text{and} \quad 0 \leq z \leq h \\ 0, & \text{elsewhere} \end{cases} \tag{3}$$

the traction free and open circuit boundary conditions ($T_{zz} = T_{xz} = T_{yz} = T_{yy} = T_{xy} = D_z = D_y = 0$ at the four boundaries) are automatically incorporated in the constitutive relations. Then, the constitutive equations can be expressed as:

$$\begin{Bmatrix} T_{xx} \\ T_{yy} \\ T_{zz} \\ T_{yz} \\ T_{xz} \\ T_{xy} \end{Bmatrix} = \begin{bmatrix} C_{11} & C_{12} & C_{13} & 0 & 0 & 0 \\ & C_{22} & C_{23} & 0 & 0 & 0 \\ & & C_{33} & 0 & 0 & 0 \\ & & & C_{44} & 0 & 0 \\ & & & & C_{55} & 0 \\ & & & & & C_{66} \end{bmatrix} \begin{Bmatrix} \varepsilon_{xx} \\ \varepsilon_{yy} \\ \varepsilon_{zz} \\ 2\varepsilon_{yz} \\ 2\varepsilon_{xz} \\ 2\varepsilon_{xy} \end{Bmatrix} I(y, z) - \begin{bmatrix} 0 & 0 & e_{31} \\ 0 & 0 & e_{32} \\ 0 & 0 & e_{33} \\ 0 & e_{24} & 0 \\ e_{15} & 0 & 0 \\ 0 & 0 & 0 \end{bmatrix} \begin{Bmatrix} E_x \\ E_y \\ E_z \end{Bmatrix} I(y, z) \tag{4a}$$

$$\begin{Bmatrix} D_x \\ D_y \\ D_z \end{Bmatrix} = \begin{bmatrix} 0 & 0 & 0 & 0 & e_{15} & 0 \\ 0 & 0 & 0 & e_{24} & 0 & 0 \\ e_{31} & e_{32} & e_{33} & 0 & 0 & 0 \end{bmatrix} \begin{Bmatrix} \epsilon_{xx} \\ \epsilon_{yy} \\ \epsilon_{zz} \\ 2\epsilon_{yz} \\ 2\epsilon_{xz} \\ 2\epsilon_{xy} \end{Bmatrix} \mathbf{I}(y,z) + \begin{bmatrix} \epsilon_{11} & 0 & 0 \\ 0 & \epsilon_{22} & 0 \\ 0 & 0 & \epsilon_{33} \end{bmatrix} \begin{Bmatrix} E_x \\ E_y \\ E_z \end{Bmatrix} \mathbf{I}(y,z) \quad (4b)$$

where C_{ij} , e_{ij} and ϵ_{ij} are the elastic, piezoelectric and dielectric coefficients respectively.

For the free harmonic plane wave propagating in x direction in a rectangular rod, we assume the displacement components to be of the form

$$u_x(x, y, z, t) = \exp(ikx - i\omega t)U(y, z) \quad (5a)$$

$$u_y(x, y, z, t) = \exp(ikx - i\omega t)V(y, z) \quad (5b)$$

$$u_z(x, y, z, t) = \exp(ikx - i\omega t)W(y, z) \quad (5c)$$

$$\phi(x, y, z, t) = \exp(ikx - i\omega t)X(y, z) \quad (5d)$$

where $U(y, z)$, $V(y, z)$, $W(y, z)$ represent the wave amplitudes in x , y and z directions respectively, and $X(y, z)$ represents the electric potential amplitude. ω is the angular frequency and k is the magnitude of the wave vector in the propagation direction.

Substituting equations (2)-(5) into equation (1), the governing differential equations in terms of displacement and electric potential components, gives:

$$\begin{aligned} & [C_{55}U_{,zz} - k^2C_{11}U + C_{66}U_{,yy} + ik(C_{12} + C_{66})V_{,y} + ik(C_{13} + C_{55})W_{,z} \\ & + ik(e_{31} + e_{15})X_{,z}] \cdot I(y, z) + C_{55}(U_{,z} + ikW + ike_{15}X)I(y, z)_{,z} \\ & + C_{66}(U_{,y} + ikV)I(y, z)_{,y} = -\rho\omega^2U \end{aligned} \quad (6a)$$

$$\begin{aligned} & [C_{44}V_{,zz} - k^2C_{66}V + C_{22}V_{,yy} + ik(C_{12} + C_{66})U_{,y} + (C_{23} + C_{44})W_{,yz} \\ & + (e_{24} + e_{32})X_{,yz}]I(y, z) + [C_{44}(V_{,z} + W_{,y}) + e_{24}X_{,y}]I(y, z)_{,z} \\ & + (ikC_{12}U + C_{22}V_{,y} + C_{23}W_{,z} + e_{32}X_{,z})I(y, z)_{,y} = -\rho\omega^2V \end{aligned} \quad (6b)$$

$$\begin{aligned} & [C_{33}W_{,zz} - k^2C_{55}W + C_{44}V_{,yy} + ik(C_{13} + C_{55})U_{,z} + (C_{23} + C_{44})W_{,yz} \\ & - k^2e_{15}X + e_{33}X_{,zz} + e_{24}X_{,yy}]I(y, z) \\ & + (ikC_{13}U + C_{23}V_{,y} + C_{33}W_{,z} + e_{33}X_{,z})I(y, z)_{,z} \\ & + C_{44}(V_{,z} + W_{,y} + e_{24}X_{,y})I(y, z)_{,y} = -\rho\omega^2W \end{aligned} \quad (6c)$$

$$\begin{aligned}
& [ik(e_{31} + e_{15})U_{,z} + ik(e_{24} + e_{32})V_{,yz} + e_{33}W_{,zz} + e_{24}W_{,yy} - k^2e_{15}W \\
& - \epsilon_{33}X_{,zz} + k^2\epsilon_{11}X - \epsilon_{22}X_{,yy}]I(y, z) \\
& + (ike_{31}U + e_{32}V_{,y} + e_{33}W_{,z} - \epsilon_{33}X_{,z})I(y, z)_{,z} \\
& + (e_{24}V_{,z} + e_{24}W_{,y} - \epsilon_{22}X_{,y})I(y, z)_{,y} = 0
\end{aligned} \tag{6d}$$

To solve the coupled wave equation (6), $U(y, z)$, $V(y, z)$, $W(y, z)$ and $X(y, z)$ are all expanded to products of two Legendre orthogonal polynomial series,

$$\begin{aligned}
U(y, z) &= \sum_{m,n=0}^{\infty} p_{m,n}^1 Q_m(z) Q_n(y), & V(y, z) &= \sum_{m,n=0}^{\infty} p_{m,n}^2 Q_m(z) Q_n(y), \\
W(y, z) &= \sum_{m,n=0}^{\infty} p_{m,n}^3 Q_m(z) Q_n(y), & X(y, z) &= \sum_{m,n=0}^{\infty} p_{m,n}^4 Q_m(z) Q_n(y)
\end{aligned} \tag{7}$$

where $p_{m,n}^i$ ($i = 1, 2, 3, 4$) are the expansion coefficients, and the orthonormal set of polynomials are

$$Q_m(z) = \sqrt{\frac{2m+1}{h}} P_m\left(\frac{2z-h}{h}\right), \quad Q_n(y) = \sqrt{\frac{2n+1}{d}} P_n\left(\frac{2y-d}{d}\right) \tag{8}$$

where P_m and P_n represent the m th and the n th Legendre polynomial respectively.

Multiplying each equation by $Q_j(y) \cdot Q_l(z) \cdot e^{-j\omega t}$ with j and l running respectively from zero to M and zero to N , and integrating over z from zero to h and y from zero to d , and taking advantage of the orthonormality of the polynomials $Q_m(z)$ and $Q_n(y)$, equation (6) can be reorganized into a form of the system problem:

$$A_{11}^{jlmn} p_{m,n}^1 + A_{12}^{jlmn} p_{m,n}^2 + A_{13}^{jlmn} p_{m,n}^3 + A_{14}^{jlmn} p_{m,n}^4 = -\omega^2 \cdot M_{jlmn} p_{m,n}^1 \tag{9a}$$

$$A_{21}^{jlmn} p_{m,n}^1 + A_{22}^{jlmn} p_{m,n}^2 + A_{23}^{jlmn} p_{m,n}^3 + A_{24}^{jlmn} p_{m,n}^4 = -\omega^2 \cdot M_{jlmn} p_{m,n}^2 \tag{9b}$$

$$A_{31}^{jlmn} p_{m,n}^1 + A_{32}^{jlmn} p_{m,n}^2 + A_{33}^{jlmn} p_{m,n}^3 + A_{34}^{jlmn} p_{m,n}^4 = -\omega^2 \cdot M_{jlmn} p_{m,n}^3 \tag{9c}$$

$$A_{41}^{jlmn} p_{m,n}^1 + A_{42}^{jlmn} p_{m,n}^2 + A_{43}^{jlmn} p_{m,n}^3 + A_{44}^{jlmn} p_{m,n}^4 = 0 \tag{9d}$$

where $A_{\alpha\beta}^{jlmn}$ ($\alpha, \beta = 1, 2, 3, 4$) and M_{jlmn} are the elements of a non-symmetric matrix. They can be obtained according to equation (6).

Equation (9d) can be written as:

$$p_{m,n}^4 = -\left(A_{44}^{jlmn}\right)^{-1} \left(A_{41}^{jlmn} p_{m,n}^1 + A_{42}^{jlmn} p_{m,n}^2 + A_{43}^{jlmn} p_{m,n}^3\right) \tag{10}$$

Substituting equation (10) into equations (9a), (9b) and (9c), gives:

$$\begin{aligned} & \left[A_{11}^{jlmn} - A_{14}^{jlmn} \left(A_{44}^{jlmn} \right)^{-1} \cdot A_{41}^{jlmn} \right] p_{m,n}^1 + \left[A_{12}^{jlmn} - A_{14}^{jlmn} \left(A_{44}^{jlmn} \right)^{-1} \cdot A_{42}^{jlmn} \right] p_{m,n}^2 \\ & + \left[A_{13}^{jlmn} - A_{14}^{jlmn} \left(A_{44}^{jlmn} \right)^{-1} \cdot A_{43}^{jlmn} \right] p_{m,n}^3 = -\omega^2 M_{jlmn} p_{m,n}^1 \end{aligned} \quad (11a)$$

$$\begin{aligned} & \left[A_{21}^{jlmn} - A_{24}^{jlmn} \left(A_{44}^{n,m} \right)^{-1} \cdot A_{41}^{jlmn} \right] p_{m,n}^1 + \left[A_{22}^{jlmn} - A_{24}^{jlmn} \left(A_{44}^{jlmn} \right)^{-1} \cdot A_{42}^{jlmn} \right] p_{m,n}^2 \\ & + \left[A_{23}^{jlmn} - A_{24}^{jlmn} \left(A_{44}^{jlmn} \right)^{-1} \cdot A_{43}^{jlmn} \right] p_{m,n}^3 = -\omega^2 M_{jlmn} p_{m,n}^1 \end{aligned} \quad (11b)$$

$$\begin{aligned} & \left[A_{31}^{jlmn} - A_{34}^{jlmn} \left(A_{44}^{jlmn} \right)^{-1} \cdot A_{41}^{jlmn} \right] p_{m,n}^1 + \left[A_{32}^{jlmn} - A_{34}^{jlmn} \left(A_{44}^{jlmn} \right)^{-1} \cdot A_{42}^{jlmn} \right] p_{m,n}^2 \\ & + \left[A_{33}^{jlmn} - A_{34}^{jlmn} \left(A_{44}^{jlmn} \right)^{-1} \cdot A_{43}^{jlmn} \right] p_{m,n}^3 = -\omega^2 M_{jlmn} p_{m,n}^1 \end{aligned} \quad (11c)$$

Then, equation (9) can be written as

$$\begin{bmatrix} \bar{A}_{11}^{jlmn} & \bar{A}_{12}^{jlmn} & \bar{A}_{13}^{jlmn} \\ \bar{A}_{21}^{jlmn} & \bar{A}_{22}^{jlmn} & \bar{A}_{23}^{jlmn} \\ \bar{A}_{31}^{jlmn} & \bar{A}_{32}^{jlmn} & \bar{A}_{33}^{jlmn} \end{bmatrix} \begin{Bmatrix} p_{m,n}^1 \\ p_{m,n}^2 \\ p_{m,n}^3 \end{Bmatrix} = -\omega^2 \begin{bmatrix} M_{jlmn} & 0 & 0 \\ 0 & M_{jlmn} & 0 \\ 0 & 0 & M_{jlmn} \end{bmatrix} \begin{Bmatrix} p_{m,n}^1 \\ p_{m,n}^2 \\ p_{m,n}^3 \end{Bmatrix}. \quad (12)$$

So, equation (12) yields a form of the eigenvalue problem. The eigenvalue ω^2 gives the angular frequency of the guided wave; eigenvectors $p_{m,n}^i$ ($i = 1, 2, 3$) allow the components of the particle displacement to be calculated, and $p_{m,n}^4$ determines the electric potential distribution. In practice, the summation of the expressions is truncated to some finite values M and N when higher-order terms become essentially negligible. According to $Vph = \omega/k$, the phase velocity can be obtained. The complex matrix equation (12) can be solved numerically making use of standard computer programs for the diagonalization of non-symmetric square matrices. $3(M+1) \cdot (N+1)$ eigenmodes are generated from the order M and N of the expansion.

3 Numerical results

Based on the foregoing formulations, computer programs in terms of the extended polynomial method have been written using Mathematica to calculate the dispersion curves and displacement distributions for the rectangular piezoelectric rods.

The physical properties of the material used in this paper, PZT-4, are listed in Table 1.

Table 1: Material parameters of the piezoelectric material ($C_{ij}/(10^{10}\text{N/m}^2), e_{ij}/(\text{C/m}^2), \epsilon_{ij}/(10^{-11}\text{F/m}), \rho/(10^3\text{kg/m}^3)$).

Parameter	C_{11}	C_{12}	C_{13}	C_{22}	C_{23}	C_{33}	C_{44}	C_{55}	C_{66}
PZT-4	13.9	7.8	7.4	13.9	7.4	11.5	2.56	2.56	3.05
	e_{15}	e_{24}	e_{31}	e_{32}	e_{33}	ϵ_{11}	ϵ_{22}	ϵ_{33}	ρ
	12.7	12.7	-5.2	-5.2	15.1	650	650	560	7.5

3.1 Approach validation

To the authors' knowledge, there are not published results on the wave propagation for rectangular piezoelectric rods so far. In order to check the effectiveness of the proposed approach and to validate our computer program, we calculate a square steel rod ($C_L = 5.85 \text{ km/s}$, $C_T = 3.23 \text{ km/s}$, $h = d = 5.08 \text{ mm}$) and make a comparison with available results obtained from the semi-analytical finite element method [Hayashi et al. (2003)]. Figure 2 is the corresponding dispersion curves, of which dotted lines are from Hayashi [Hayashi et al. (2003)], and dashed lines are from the proposed polynomial approach. As can be seen, the agreement between polynomial approach and the available results is quite good.

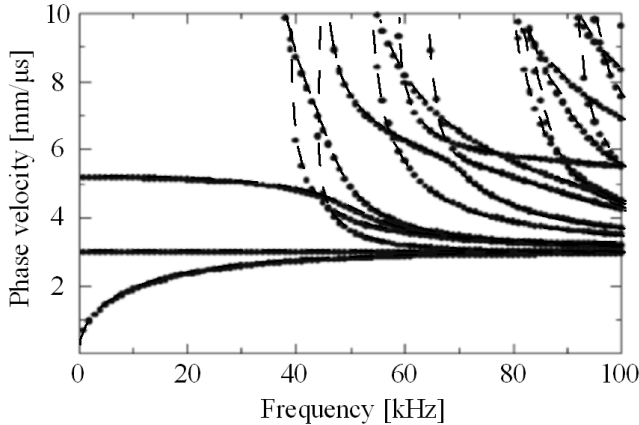


Figure 2: Phase velocity dispersion curves of the square steel rod; dotted lines: Hayashi's results, dashed lines: authors' results.

3.2 Guided wave in rectangular piezoelectric rods

Figure 3 shows the dispersion curves of the PZT-4 rod and of the corresponding non-piezoelectric one with $d = h = 1\text{mm}$. It can be seen that piezoelectricity has a significant effect on the dispersion curves. For any one specific mode, the phase velocities of piezoelectric rod are bigger than those of the corresponding non-piezoelectric rod, and the piezoelectric effect becomes stronger with the wave number increasing. In micro-scale SAW devices, the wave number is usually very big and the operating frequency is very high. So, the piezoelectric effects will be prominent.

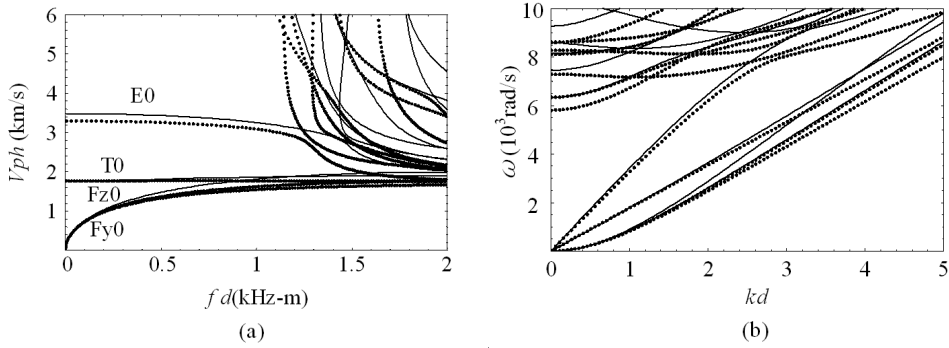


Figure 3: Dispersion curves of the square PZT-4 rod: (a) phase velocity spectra, (b) frequency spectra, solid line, piezoelectric; dotted line, non-piezoelectric.

There are two symmetry axes (y and z axes) for guided wave in rectangular rods. According to displacement distribution in wave propagating direction (displacement u), the wave modes can be classified into four kinds: flexure y modes (Fy modes: sym- y /asym- z), flexure z modes (Fz modes: asym- y /sym- z), extension modes (E modes: sym- y /sym- z) and torsion modes (T modes: asym- z /asym- y). The first order modes of the four modes are marked in Figure 3. Figures 4-7 give, for the square piezoelectric rod, the displacement distributions of the first four modes at $kd=2$. For Fz0 mode, displacement v is sym- y /sym- z and w is asym- y /asym- z . For Fy0 mode, displacement v is asym- y /asym- z and w is sym- y /sym- z . For E0 mode, displacement v is asym- y /sym- z and w is sym- y /asym- z . For T0 mode, displacement v is sym- y /asym- z and w is asym- y /sym- z . The symmetric cases of the displacements for higher modes are the same as the corresponding ones for the low modes. The electric potential of all modes have the same symmetry to the corresponding displacement w . The case of big wavenumber is also given. Figures

8 and 9 show the displacement and electric potential distributions of Fy_0 mode and T_0 mode at $kd=150$, respectively. It can be seen that the symmetric cases of big wavenumber are the same to the ones of small wavenumber, and the displacement w and electric potential of the rod at big wavenumber always distribute around the four boundaries.

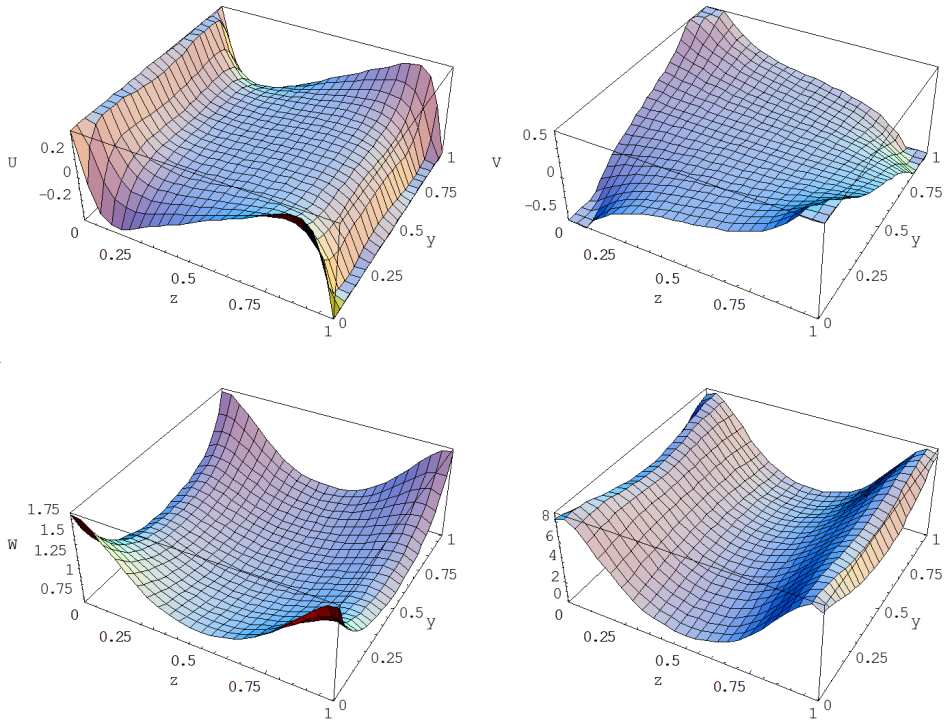


Figure 4: Displacement and electric potential profiles of Fy_0 mode at $kd=2$.

Figure 1 shows the dispersion curves of the rectangular PZT-4 rods with different height to width ratios, $d/h=1/2$, $d/h=2$ and $d/h=4$. It can be seen that the width to height ratio has a significant influence on the dispersion curves. For the rectangular piezoelectric rod, the first four wave modes have no cut-off frequencies, which is different from that for an infinite flat plate in which only the first two modes have no cut-off frequencies.

Figure 11 shows the dispersion curves of the first six modes of the square PZT-4 rod with polarization in x direction. In order to illustrate the effect of the polarization direction on the dispersion curves, we keep the elastic constants invariable, and

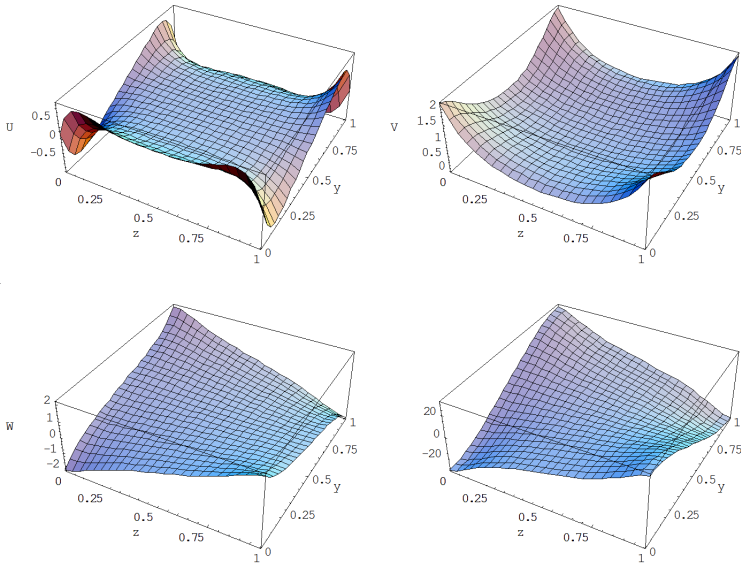


Figure 5: Displacement and electric potential profiles of Fz0 mode at $kd=2$.

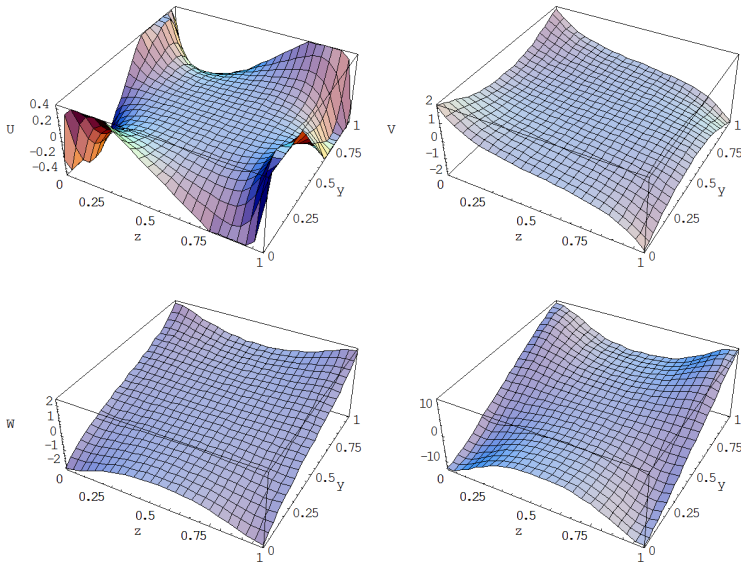


Figure 6: Displacement and electric potential profiles of T0 mode at $kd=2$.

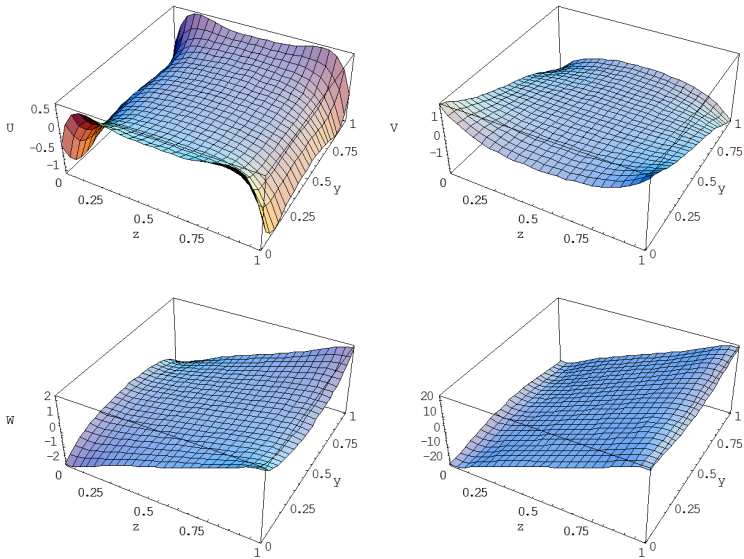


Figure 7: Displacement and electric potential profiles of E0 mode at $kd=2$.

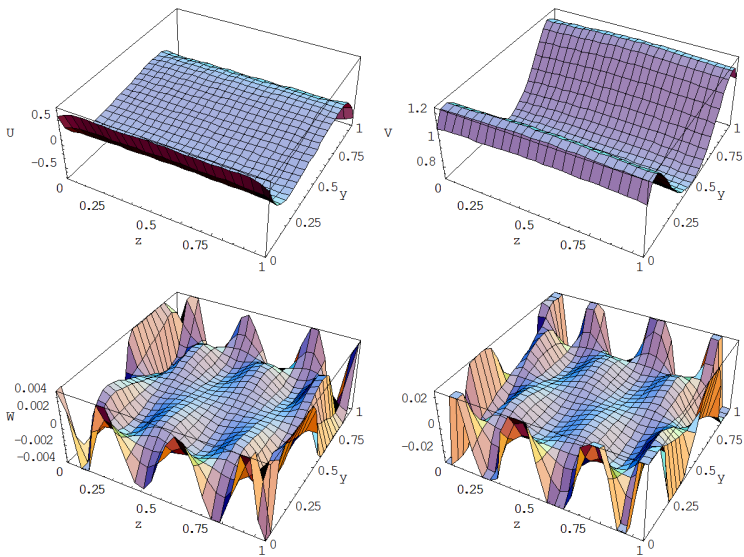


Figure 8: Displacement and electric potential profiles of Fz0 mode at $kd=150$.

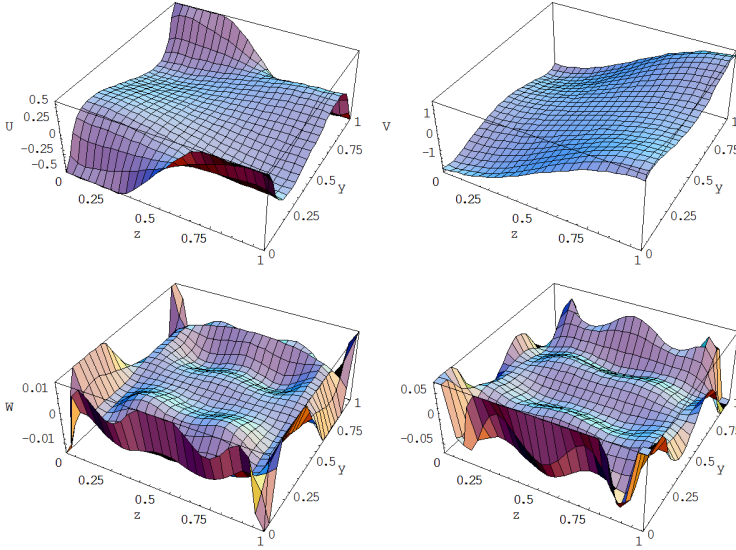


Figure 9: Displacement and electric potential profiles of T0 mode at $kd=150$.

piezoelectric constants become $e_{11} = 15.1$, $e_{12} = e_{13} = -5.2$, $e_{26} = e_{35} = 12.7$ and dielectric constants become $\epsilon_{11} = \epsilon_{33} = 650$, $\epsilon_{22} = 560$. It can be seen that piezoelectricity has a significant effect on the high order modes and a very little effect on the first three modes. The effect of the piezoelectricity becomes strong with the order modes increasing at low frequency and becomes weak with frequency and wave number increasing, which is different from the square PZT-4 rods with polarization in y or z direction.

4 Conclusions

The formulation to analyze the guided wave propagation in 2D rectangular piezoelectric rods by using the extended orthogonal polynomial approach has been presented in this paper. The effectiveness of the proposed approach was checked by calculating a square steel rod. The dispersion curves and displacement, electric potential distributions of various rectangular piezoelectric rods are presented and discussed. According to the numerical results, we can draw the following conclusions:

- The piezoelectricity has a significant effect on the dispersion curves. The piezoelectric constants and dielectric constants have opposite influence on the piezoelectric effect.

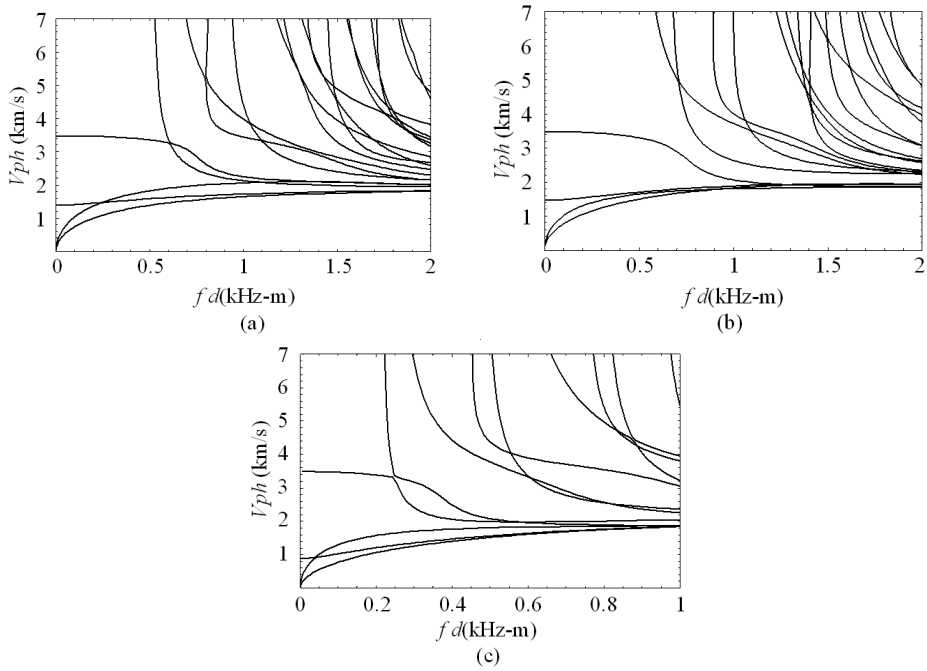


Figure 10: Phase velocity dispersion curves of the rectangular PZT-4 rods with different height to width ratios, (a) $d/h=0.5$, (b) $d/h=2$, (c) $d/h=4$.

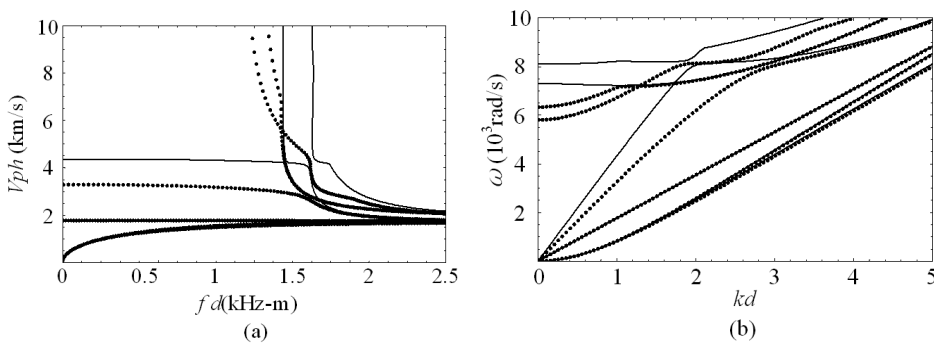


Figure 11: Dispersion curves of the square PZT-4 rod with polarization in x -direction: (a) phase velocity spectra, (b) frequency spectra, solid line, piezoelectric; dotted line, non-piezoelectric.

- The width to height ratio has a significant influence on the guided wave characteristics of piezoelectric rods with rectangular cross sections.
- The electric potential has the same symmetry to the corresponding displacement w for all modes. The electric potential of the piezoelectric rod with rectangular cross sections at big wavenumber always distribute around the four boundaries.
- The effects of the different polarization direction on the guided wave in rectangular piezoelectric rods are different.
- We believe that the proposed method could be of interest in non destructive testing evaluation and also to deal with various multi-field coupled 2D structures, such as in magneto-electro-elastic 2D structures, and deal with inhomogeneous structures, such as multilayered and graded 2D structures.

Acknowledgment: The work is supported by the National Natural Science Foundation of China (No. 11272115) and Foundation for Distinguished Young Scholars of Henan Polytechnic University (No.J2013-08) and by the high-performance grid computing platform of Henan Polytechnic University.

References

- Cai C.; Liu G. R.; Lam K. Y.** (2001): A technique for modelling multiple piezoelectric layers. *Smart Materials and Structures*, vol. 10, pp. 689-694.
- Chakraborty, A.** (2009): Wave Propagation in Porous Piezoelectric Media. *Computer Modeling in Engineering & Sciences*, vol. 40, no.2, pp. 105-132.
- Datta, S.; Hunsinger, B. J.** (1978): Analysis of surface waves using orthogonal functions. *Journal of Applied Physics*, vol. 49, pp. 475-479.
- Ebenezer, D. D.; Ramesh, R.** (2003): Analysis of axially polarized piezoelectric cylinders with arbitrary boundary conditions on the flat surfaces. *Journal of the Acoustical Society of America*, vol. 113, no.4, pp. 1900-1908.
- Guo, Y. Q.; Chen, W. Q; Zhang, Y. L.** (2009): Guided wave propagation in multilayered piezoelectric structures. *Science in China Series G: Physics, Mechanics and Astronomy*, vol. 52, no.7, pp. 1094-1104.
- Gubernatis, J. E.; Maradudin, A. A.** (1987): A Laguerre series approach to the calculation of wave properties for surfaces of inhomogeneous elastic materials. *Wave Motion*, vol. 9, pp. 111-121.
- Han, X.; Liu, G. R.; Ohyoshi, T.** (2004): Dispersion and characteristic surfaces of waves in hybrid multilayered piezoelectric circular cylinders. *Computational*

Mechanics, vol. 33, no.5, pp. 334-344.

Han, X.; Ding, H.; Liu, G. R. (2005): Elastic waves in a hybrid multilayered piezoelectric plate. *Computer Modeling in Engineering & Sciences*, vol. 9, no.1, pp. 49-56.

Hayashi, T.; Song, W. J.; Rose, J. L. (2003): Guided wave dispersion curves for a bar with an arbitrary cross-section, a rod and rail example. *Ultrasonics*, vol. 41, no.3, pp. 175-183.

Ing, Y. S.; Liao, H. F.; Huang, K. S. (2013): The extended Durbin method and its application for piezoelectric wave propagation problems. *International Journal of Solids and Structures*, vol. 50, no.24, pp. 4000-4009.

Kim, Y.; Hunt, W. D. (1990): Acoustic fields and velocities for surface-acoustic-wave propagation in multilayered structures: An extension of the Laguerre polynomial approach. *Journal of Applied Physics*, vol. 68, pp. 4993-4997.

Lefebvre, J. E.; Zhang, V.; Gazalet, J.; Gryba, T. (1999): Legendre polynomial approach for modeling free ultrasonic waves in multilayered plates. *Journal of Applied Physics*, vol. 85, pp. 3419-3427.

Lefebvre, J. E.; Zhang, V.; Gazalet, J.; Gryba, T.; Sadaune, V. (2001): Acoustic wave propagation in continuous functionally graded plates: An extension of the Legendre polynomial approach. *IEEE Transactions on Ultrasonics Ferroelectrics and Frequency Control*, vol. 48, pp. 1332-1340.

Liu, G. R.; Dai, K. Y.; Han, X.; Ohyoshi, T. (2003): Dispersion of waves and characteristic wave surfaces in functionally graded piezoelectric plates. *Journal of Sound and Vibration*, vol. 268, no.1, pp. 131-147.

Maradudin, A. A.; Wallis, R. F.; Mills, D. L.; Ballard, R. L. (1972): Vibrational edge modes in finite crystals. *Physical Review B*, vol. 6, pp. 1106-1111.

Paul, H. S.; Venkatesan, M. (1987): Wave propagation in a piezoelectric solid cylinder of arbitrary cross section. *Journal of the Acoustical Society of America*, vol. 82, pp. 2013-2020.

Sharon, T. M.; Maradudin, A. A.; Cunningham, S. L. (1974): Vibrational modes on a rectangular ridge. *Letters in Applied and Engineering Sciences*, vol. 2, pp. 161-174.

Wu, B.; Yu, J. G.; He, C. F. (2008): Wave propagation in non-homogeneous magneto-electro-elastic plates. *Journal of sound and vibration*, vol. 317, pp. 250-264.

Xi, Z. C.; Liu, G. R.; Lam, K. Y.; Shang, H. M. (2002): Dispersion of waves in immersed laminated composite hollow cylinders. *Journal of Sound and Vibration*, vol. 250, pp. 215-227.

Yu J. G.; Lefebvre J. E.; Guo Y. Q.; Elmaimouni L. (2012): Wave propagation in the circumferential direction of general multilayered piezoelectric cylindrical plates. *IEEE T. Ultrasonics, Ferroelectrics and Frequency Control*, vol. 59, no.11, pp. 2498-2508

Yu J. G.; Lefebvre J. E. ; Guo Y. Q. (2013): Wave propagation in multilayered piezoelectric spherical plates. *Acta Mechanica* vol. 224, no.7, pp. 1335-1349

Yu, J. G.; Ma, Q. J.; Su, S. (2008): Wave propagation in non-homogeneous magneto-electro-elastic hollow cylinders. *Ultrasonics* vol. 48, no.8, pp. 664-677

Yu, J. G.; Ma, Q. J. (2010): Wave characteristics in magneto-electro-elastic functionally graded spherical curved plates. *Mechanics of Advanced Materials and Structures*, vol. 17, no.4, pp. 287-301.

